Biocompatible blood pool MRI contrast agents based on hyaluronan

Wenlian Zhu[a] and **Dmitri Artemov**[a,*]

[a] JHU ICMIC Program, The Russell H. Morgan Department of Radiology and Radiological Science, Johns Hopkins University School of Medicine, Baltimore, MD 21205, USA

Abstract

Biocompatible gadolinium blood pool contrast agents based on a biopolymer, hyaluronan, were investigated for magnetic resonance angiography application. Hyaluronan, a non-sulfated linear glucosaminoglycan composed of 2000–25,000 repeating disaccharide subunits of D-glucuronic acid and *N*-acetylglucosamine with molecular weight up to 20 MDa, is a major component of the extracellular matrix. Two gadolinium contrast agents based on 16 and 74 kDa hyaluronan were synthesized, both with R_1 relaxivity around 5 mM^{-1} s^{-1} per gadolinium at 9.4 T at 25°C. These two hyaluronan based agents show significant enhancement of the vasculature for an extended period of time. Initial excretion was primarily through the renal system. Later uptake was observed in the stomach and lower gastrointestinal tract. Macromolecular hyaluronan-based gadolinium agents have a high clinical translation potential as hyaluronan is already approved by FDA for a variety of medical applications.

Keywords

hyaluronan; biocompatible contrast agents; magnetic resonance angiography

1. INTRODUCTION

Blood pool contrast agents (BPCA) are desirable in applications such as magnetic resonance angiography (MRA) and tumor microvasculature characterization. In comparison to the commonly used extracellular MRI contrast agents such as gadopentetate dimeglumine, BPCAs exhibit lower leakage into the interstitial space, which minimizes non-specific soft tissue enhancement while prolonging the plasma half-life. These characteristics, in combination with higher relaxivity, can provide better contrast for blood vessels as compared with the standard small molecular extracellular contrast agents. Relative to normal tissues, solid tumors have enhanced permeability and retention of macromolecules (1). Thus, macromolecules-based contrast agents are also well suited to assessing tumor angiogenesis due to these tumor-specific properties.

To attain prolonged blood circulation time, gadolinium containing BPCAs are designed as either small molecules that bind to serum albumin, or macromolecules. Currently, there is only one blood pool MRI contrast agent, gadofosveset trisodium, that has been approved for clinical MRA application in Europe (2). Gadofosveset trisodium is also approved by the FDA in the United States to evaluate aortoiliac occlusive disease in adults with known or suspected peripheral vascular complication. Gadofosveset trisodium is a small molecule that

reversibly binds to blood serum albumin, which has been proven to be beneficial for MRA applications. However, the properties of macromolecular BPCAs make them better suited for studies aimed at quantifying tumor microvasculature as ambiguities related to reversible albumin binding dynamics are avoided (3). Many macromolecular blood pool agents under current development have shortcomings because of a lack of biocompatibility, toxicity, immunogenicity (4,5) and slow excretion, which eventually can result in the accumulation of toxic Gd^{3+} ions (6–8). An ideal macromolecular BPCA needs to be large enough so that it has a prolonged blood circulation time and yet small enough to pass through the kidney for unhindered excretion. It has been reported that the vascular permeability in normal tissues of macromolecules with molecular weights greater than 50 kDa is very limited, while the ultrafiltration threshold of the kidney glomerular membrane is below the size of blood serum albumin, a globular protein of 67 kDa (9). If the molecular size was the only determining factor, it would appear that molecules with molecular weight between 50 and 65 kDa would be most suitable blood pool contrast agent candidates. They would remain in the circulation for an extended period of time, and eventually would be eliminated through the kidneys. However, other factors, such as charge, shape and hydrophilic/lipophilic balance also affect the extravasation and excretion rates of macromolecules. Generally, amphipathic organic anions with a relatively high molecular weight are eliminated by the liver via metabolism and/or biliary excretion while small and hydrophilic organic anions are excreted into the urine (10). Relatively unhindered clearance through the kidneys may be achieved by using hydrophilic agents with limited protein binding.

Hyaluronan (HA) is a suitable macromolecule platform for developing blood pool contrast agents. HA is a natural linear polysaccharide composed of alternating (β-1,4)-linked D-glucuronic acid and (β-1,3) N-acetyl-D-glucosamine residues with molecular weights as high as 10^7 Da. HA is widely distributed in the extracellular matrix of connective tissues of animals and plays a role in organ structural stability and tissue organization. It is biocompatible and non-immunogenic. HA is readily available in a wide range of defined molecular weights through microbial fermentation (11,12). Because of its unique viscoelastic rheological properties and safety profile, HA has been utilized in a broad range of medical applications such as ophthalmology, orthopedic surgery and rheumatology, otolaryngology, dermatology and plastic surgery, surgery and wound healing, and pharmacology and drug delivery (13). More significantly, Hyaluronic Acid Chemotransport Technology (HyACT®), in which anti-cancer drugs are entrained in an HA matrix, has entered human clinical trials (14). There is also great interest in using HA as a drug carrier and a ligand on liposomes or nanoparticles to target CD44 overexpressing cancer cells. Esposito *et al.* have reported that the uptake of HA-functionalized Gd-liposomes in various tumor cells was directly proportional to their expression levels of CD44 receptors (15). Drugs delivered in HA-modified liposomes exhibited excellent antitumor activity both in vitro and in murine tumor models (16). HA is naturally biodegradable since it is digested by a series of enzymatic reactions *in-vivo* that generate polysaccharides of decreasing sizes, which in principle may facilitate the timely excretion of HA-based macromolecular contrast agents. In this study, we used HA of molecular weight 16 and 74 kDa, which contain approximately 40 and 183 repeating disaccharide subunits, respectively, as macromolecular backbone carriers for Gd–DTPA groups. We assessed the enhancement pattern of these HA and Gd–DTPA complex as blood pool agents, and compared them with another common preclinical macro-molecular blood pool MRI contrast agent, a bovine serum albumin Gd–DTPA complex (17,18).

2. MATERIALS AND METHODS

2.1. Materials

Hyaluronan with molecular weights of 16 and 74 kDa was obtained from Lifecore Biomedical (Chaska, Minnesota). *N*-(3-dimethylaminopropyl)-*N*-ethylcarbodiimide hydrochloride (EDC) and *N*-hydroxysuccinimide (NHS) were from Pierce (Rock-ford, IL, USA). Other reagents were obtained from Sigma-Aldrich (St Louis, MO, USA). All reagents were used without further purification. SCID mice were purchased from NCI with body weight ranged from 21 to 25 g.

2.2. Synthesis of hyaluronan–ethylenediamine–diethylenetriaminepentaacetic acid–gadolinium (HA–EDA–DTPA–Gd)

HA–(EDA–Gd–DTPA) was synthesized with a modified method described previously (19,20). All conjugation reactions were carried out at room temperature. Briefly, 200 mg of HA of different molecular weights (0.5 mmol of disaccharide monomer subunit) was dissolved in 2-(*N*-morpholino)ethanesulfonic acid buffer (MES, 0.1 mol/L, 20 mL, pH 4.75). The carboxyl groups of hyaluronan were activated by the addition of 200 mg (1.04 mmol) EDC and 80 mg (0.70 mmol) NHS for 30 min. A 200 mg (3.3 mmol) aliquot of ethylenediamine (EDA) was added to this activated hyaluronan solution while pH was maintained at 7.0 with the addition of 1 M HCl. This solution was stirred at room temperature for 3 h. The product, HA–EDA conjugate, was purified by ultra-filtration with an Amicon Centrifugal unit with a 5 or 10 kDa membrane. Hyaluronan–EDA conjugate was subsequently reacted with 200 mg (0.56 mmol) solid DTPA dianhydride in three additions in 40 ml 0.1 M HEPES buffer while pH was maintained at around 10 with the addition of 1 M NaOH. This solution was stirred overnight at room temperature. A second batch of 200 mg solid DTPA anhydride was added the next day and the reaction proceeded for a further 3 h. The product, HA–(EDA–DTPA) conjugate, was purified through ultrafiltration with water multiple times. Chelating of gadolinium was performed with the addition of 500 mg solid $GdCl_3 \cdot 6H_2O$ (1.3 mmol). This reaction proceeded overnight at pH 7 in 0.1 M citric acid buffer. Final product HA–(EDA–DTPA–Gd) was purified through exhaustive ultra filtration with water and lyophilized. The absence of free Gd^{3+} in the final product was confirmed by an arsenazo III assay (20).

2.3. T_1 measurement of HA–(EDA–DTPA–Gd) conjugates

T_1 values of the HA–(EDA–DTPA–Gd) conjugates were measured in deionized water at 25°C. T_1 measurements were performed on a horizontal 9.4 T Bruker Biospec spectrometer using an inversion–recovery ($180 - \tau - 90$ sequence) method with a fixed T_R of 2000 ms and nine varying delays of 5, 10, 20, 50, 100, 200, 500, 1000 and 2000 ms. T_1 values were calculated by IDL (Interactive Data Language) using mono-exponential fittings with a linear least-square regression of the FID amplitude. T_1 measurements were also performed on a clinical 1.5 T GE Signa scanner using saturation–recovery spin echo imaging with echo time at 9 ms and varying recovery delays of 100, 200, 400, 800 and 1600 ms. T_1 values were calculated using mono-exponential fittings with a linear least-square regression of the image amplitudes.

2.4. ICP-MS measurements

Gadolinium content of the HA–(EDA–DTPA–Gd) conjugates was determined by inductively coupled plasma mass spectroscopy (ICP-MS). HA–(EDA–DTPA–Gd) conjugates were dissolved in 2% element analysis grade nitric acid and diluted to the ICP-MS measurement range, from 5 to 40 μg/L. The gadolinium concentration of this diluted

solution was calibrated with a series of ICP-MS standard gadolinium solutions within the same range.

2.5. Stability measurements

HA–(EDA–DTPA–Gd) conjugates based on 16 kDa HA at the concentration of 4 mg ml^{-1} (Gd concentration 1.1 mM) were incubated in RPMI medium that contains 10% fetal bovine serum at pH 6.4, 7.4, and 9.0 respectively over 5 days at 37°C, while T_1 values of these solutions were measured at 25°C at various time points.

2.6. In vivo MRA studies

All animal experiments were performed in accordance with institutional guidelines. *In vivo* MRA experiments were performed on a horizontal 9.4 T Bruker Biospec spectrometer using a circular volume coil. Mice were anesthetized with an intraperitoneal (i.p.) injection of a ketamine–acepromazine mixture (25 and 2.5 mg kg^{-1}, respectively, in saline) prior to all procedures. For magnetic resonance angiography studies, the tail vein of the mice was catheterized with a 25G needle, which was connected to a T-shape connector that was attached to a HA–(EDA–DTPA–Gd) syringe on one side and a saline syringe (plus 10 i.u. heparin) on the other side. Each syringe was fitted with a stopcock outside the magnet via a 50 cm polyethylene (PE60) catheter tube. HA–(EDA–DTPA–Gd) was given at a dose of 0.1 mmolGd kg^{-1}. For comparison, BSA-(DTPA–Gd) was also given at a dose of 0.1 mmolGd kg^{-1}. After a triplanar orthogonal scout imaging of the whole body, coronal MRA images were acquired with a three-dimensional fast low-angle shot (FLASH) MR sequence (flip angle 45°, echo time/repetition time 1.85 ms/8 ms, FOV 60 × 26 × 26 mm, matrix 128 × 64 × 64, number of averages 8) before and after the administration of the contrast agent. The total acquisition time was 4 min 30 s. Data analysis was performed using software developed by the IDL program environment. After 3D apodization and Fourier transformation, all final matrices were zero filled to 256 × 128 × 128. Data visualization was through ImageJ (NIH) and Amira (Visage Imaging).

2.7. Blood half-life studies

Mice were anesthetized with an intraperitoneal (i.p.) injection of a ketamine–acepromazine mixture. HA–(EDA–DTPA–Gd) based on 16 kDa HA at a dose of 0.05 mmol Gd kg^{-1} was injected through the mouse tail vein. About 20 µl of blood was drawn from the tail vein and collected into a dry and heparinized PCR tube at each time point. T_1 of these blood samples were measured by an inversion recovery method at 25°C. Intrinsic blood T_1 was measured prior to the administration of the contrast agent. The increase of relaxation rate due to HA–(EDA–DTPA–Gd) was obtained after the subtraction of the intrinsic blood relaxation rate from the total blood relaxation rate at each time point. Fast clearance and slow clearance half-life were calculated with a two phase decay model after the intrinsic blood rate was subtracted.

3. RESULTS

3.1. T_1 values

T_1 values and corresponding relaxivity of HA–(EDA–DTPA–Gd) prepared from HA of molecular weight 16 and 74 kDa in deionized water at 1.5 and 9.4 T at 25°C are shown in Table 1. Relaxivity of the individual conjugate was calculated based on these T_1 values, HA–(EDA–DTPA–Gd) concentration and gadolinium content and water relaxation time of 2.5 and 2.8 s at 1.5 and 9.4 T.

3.2. Gadolinium content of HA–(EDA–DTPA–Gd) conjugates

The gadolinium content of each HA–(EDA–DTPA–Gd) conjugate varied slightly with preparations as observed by its T_1 values. The gadolinium content of the conjugates based on 16 and 74 kDa HA used in this report was around 5% of the total weight as determined by ICP-MS, shown in Table 1, which corresponds to about one in every six HA carboxyl groups conjugated to (EDA–DTPA–Gd) and increased the nominal molecular weight of final complexes from 16 and 74 kDa to about 21 and 95 kDa, respectively (see Supporting Information[Q1]).

3.3. Stability

T_1 values of the HA–(EDA–DTPA–Gd) conjugate based on 16 kDa HA in RPMI medium with 10% serum were measured within 5 min and up to 5 days at pH 6.3, 7.4 and 9.0. About a 5% increase in T_1 was observed at 24 h in all three pH conditions, and up to 14% increase in T_1 was observed in 5 days, Table 2.

3.4. In vivo MRI studies

Figure 1 shows a time series of maximal intensity projection (MIP) of the coronal 3D FLASH images obtained from the mice injected with HA–(EDA–DTPA–Gd) based on 16 and 74 kDa HA. The time label of each image is listed as that of the beginning of the acquisition after the injection, and pre-contrast images were subtracted from post-contrast images. For comparison, results from BSA-(DTPA–Gd), a well tested blood pool contrast agent given at the same gadolinium dose, are also shown in Fig. 2. Initially, intense and prolonged enhancement was observed in the vasculature for both HA–(EDA–DTPA–Gd) conjugates and BSA-(DTPA–Gd). However, different distribution and excretion patterns emerged over the next 30 min. For HA–(EDA–DTPA–Gd), the distribution of the contrast was initially limited to the blood vessels. HA–(EDA–DTPA–Gd) prepared from HA of molecular weight 74 kDa showed greater detail of the circulatory system, especially in the liver and spleen. Marked washout was seen for HA–(EDA–DTPA–Gd) prepared from 16 kDa HA after 10 min while the washout was barely noticeable for the 74 kDa agent, even at 30 min (Fig. 1). These agents were readily excreted through the kidney to the bladder. HA–(EDA–DTPA–Gd) of lower molecular weight appeared to be excreted through the kidney faster than its counter part of higher molecular weight as shown in Fig. 3, images taken 150 min after the injection: aorta and vena cava were barely visible for the agent based on 16 kDa while they were still enhanced for the 74 kDa agent. In contrast, no excretion to the bladder was observed for BSA–(DTPA–Gd), which leaked to the extravascular space and eventually into the tissues, especially liver and kidney at 30 min post injection. However, HA–(EDA–DTPA–Gd) showed significant uptake by the stomach. HA–(EDA–DTPA–Gd) based on 16 kDa HA was absorbed by the stomach faster than that of 74 kDa. Uptake of 16kDa HA–(EDA–DTPA–Gd) by the stomach was observed as early as 1 h post injection, and it was seen in feces 7 h later (Fig. 4). At 24 h the 16 kDa HA–(EDA–DTPA–Gd) had mostly been cleared from the stomach into the lower gastrointestinal tract and feces while significant uptake at the stomach was still observed for the 74 kDa HA–(EDA–DTPA–Gd) conjugate (Fig. 5). Overall, no adverse reactions such as weight loss and death were observed in any mice that received HA–(EDA–DTPA–Gd) conjugates within next 2 months.

3.5. Half-life of HA–(EDA–DTPA–Gd) based on 16 kDa

Figure 6 shows the blood relaxation rate of a mouse injected with HA–(EDA–DTPA–Gd) based on 16 kDa HA at various time points after the injection. The change in blood relaxation rate as a function of time is best fitted with a two-compartment pharmacokinetic model. The fast phase half-life is 12.4 min and the slow phase half-life is 141 min. Over 64% of the injected 16 kDa HA–(EDA–DTPA–Gd) was cleared during the fast phase. We

only measured the half-life of HA–(EDA–DTPA–Gd) based on 16 kDa as it may be a more suitable candidate for clinical translation due to its moderate clearance profile.

4. DISCUSSION

Since native HA does not have any modifiable amine group, conjugation of DTPA to the carboxyl group of HA was preceded by the introduction of an EDA molecule, a homobifunctional crosslinker with two amine groups. However, following the previously published EDC mediated EDA and HA conjugation methods (19,20), we were not able to obtain a final compound with adequate gadolinium content for angiography application. To boost the conjugation between the amine groups of EDA and the carboxyl groups of HA, NHS was added to the HA/EDC solution prior to EDA. Additionally, the amount of EDC added was increased to around two molecular equivalent of HA monomer unit. This process was rather efficient under our experimental conditions, as demonstrated by the gadolinium contents and T_1 relaxation time of the HA–(EDA–DTPA–Gd) solutions. Although EDA possesses two identical amine groups, the remaining free amine group becomes a weaker base upon the formation of an amide bond at the other amine group with a carboxyl group. The resulting different pK_a (6.86 and 9.92, *Handbook of Chemistry and Physics*[Q2]) most likely prevented the inter- or intra-crosslinking of two HA carboxyl groups by EDA. After one amine group of the EDA molecule is coupled to a carboxyl group of HA molecule, the second EDA amine group with pK_a of 6.86 is much less likely to be reactive towards another HA carboxyl group at our reaction condition, pH 7. The amount of EDC added to activate the HA carboxyl group is crucial for the high conjugation rate of EDA to HA. Insufficient amount of EDC drastically decreased the EDA–HA conjugation efficiency, and excess amount of EDC increased the amount of a stable abduct formed between EDC and HA (21), thus preventing the subsequent conjugation between EDA and HA.

HA–(EDA–DTPA–Gd) prepared from different molecular weights of HA (16 and 74 kDa) showed comparable gadolinium content, T_1 values at the same concentration of 1.3 mg ml^{-1} and relaxivity at 1.5 and 9.4 T respectively (Table 1). For the given concentration of 1.3 mg ml^{-1}, HA–(EDA–DTPA–Gd) prepared from different molecular weights of HA would contain the same number of disaccharide subunits, and thus the same number of gadolinium attached since the gadolinium content is nearly the same. It appeared that the T_1 relaxation rate of the HA–(EDA–DTPA–Gd) conjugates was determined by the amount of gadolinium present, and not by the molecular weight of the HA carriers at both 1.5 and 9.4 T. HA is a linear polymer of repeating disaccharide subunits. An HA molecule assumes an expanded stiffened yet flexible random coil structure in physiological solutions (22), and does not conform to a well-defined globular tertiary structure (23). Consequently, molecular weight of HA seems to have very little effect on the correlation time of the highly mobile Gd–DTPA groups and the final relaxivity of the whole conjugate in the molecular weight range used, from 16 to 74 kDa, measured at 1.5 and 9.4 T.

Nevertheless, the molecular weight of HA does affect the vascular enhancement pattern of HA–(EDA–DTPA–Gd) conjugates. The higher molecular weight agents provided a stronger and more sustained enhancement of the smaller vessels while the lower molecular weight agents exhibited a faster clearance rate through the kidney. BSA-(DTPA–Gd) was not cleared through the kidney since a normal healthy kidney is able to retain globular proteins with molecular mass above 60 kDa. Despite a higher molecular weight than BSA, HA–(EDA–DTPA–Gd) prepared from HA of 74 kDa was partially cleared from the kidney, most likely due to its linear structure, which results in an elongated random coil tertiary structure compared with globular proteins of similar molecular weight. However, HA of higher molecular weight with longer coil did result in a slower kidney excretion, compared with the lower molecular weight counterpart as shown in Fig. 1 at 30 min, and in Fig. 3 at 150 min

after the administration of the contrast agents. It is not clear how hyaluronidase, which degrades hyaluronan into lower molecular weight fragments (24), affects the clearance of HA–(EDA–DTPA–Gd). Degradation of HA by hyaluronidase is a cellular process that depends on HA receptor such as CD44 (25) or LYVE-1(26). Much of this degradation happens in lymph nodes (26) or liver (27) under normal physiological conditions. Hyaluronidase activity may well be limited when HA–(EDA–DTPA–Gd) remains in the blood circulation. Shiftan *et al* have reported using a hyaluronan–GdDTPA–agarose bead construct to detect the enhanced hyaluronidase activity of cancer cells by MRI through subcutaneous injection in the vicinity of ES-2 ovarian carcinoma tumor xenografts (19).

The *in-vivo* blood distribution of HA–(EDA–DTPA–Gd) based on 16kDa HA followed a biphasic pattern, with a fast phase half-life of 12.4 min and a slow phase half-life of 141 min. These results were consistent with the MRA studies: a fast wash-out of this contrast from the vasculature in 10 min was observed. In comparison, some common extracellular gadolinium agents such as Gd–DTPA have a distribution half-life of about 5 min and half elimination time of 80 min in human (28). Initial fast blood clearance of HA–(EDA–DTPA–Gd) was probably due to the renal excretion. Overtime, HA–(EDA–DTPA–Gd) leaked into the extra-vascular space such as stomach and the lower gastrointestinal tract and elimination entered a slow phase.

HA–(EDA–DTPA–Gd) based on 16 kDa HA is fairly stable in serum containing RPMI medium in various pH as shown in Table 2. About 5 and 14% increases in the T_1 values were observed at 24 h and 5 days, which implied that a minor amount of gadolinium was lost from the conjugate during these periods. This loss is consistent with the stability commonly observed for the DTPA–Gd macromolecular complex prepared from cyclic DTPA dianhydride (8,29). The stability of gadolinium-containing blood pool agents may be improved by the use of backbone-modified DTPA analogs in place of DTPA dianhydride, wherein all five carboxyl groups remained free for metal binding after conjugation to the macromolecules or macrocyclic chelators (8).

Stomach and lower gastrointestinal uptake of HA–(EDA–DTPA–Gd) was not expected. In general, liver and spleen were considered the organs that were involved in the HA metabolism (14). Studies of ^{3}H labeled HA intravenously injected into sheep showed a concentration-dependent half-life ranging from 5 to 44 minutes (30). It was also reported that the clearance of ^{3}H labeled HA was retarded by prior injection of excess unlabelled HA, and renal excretion with an upper limit of 25 kDa played a negligible part in clearance, and the liver was the main site of uptake (31). Fluorescence-labeled-hyaluronan with molecular weight of 800 kDa was reported to have a half-life of 42 min while the liver was shown to play a significant rule in its elimination (32). After intravenous injection of a bolus dose of ^{14}C-HA in rabbits, it was shown that 98% of the administered dose had disappeared from the systemic circulation within 6 h after the administration. Within 100 h, 63 and 20% of the administered dose was excreted and recovered in the respiratory gas (as [14]CO_2) or in urine (as low molecular weight HA or monosaccharide fragments). The same authors also reported that the total amount of excretion into bile within 24 h was reported to be very low, 0.7% of the administered dose, and the total amount of excretion HA into feces, within 100 h of administration, was also very small, about 0.5% of the administered dose (25,27). Research on the effects of size and dose of fluorescein-labeled HA on its metabolism has shown that 60% of the tail vein injected 90 kDa HA accumulated in the liver, while both the 3 and 10 kDa fluorescein-labeled HA were quickly excreted in urine with no accumulation in any tissues (33). With gadolinium content at 5% by weight, HA–(EDA–DTPA–Gd) based on 16 and 74 kDa would have a nominal molecular weight around 21 kDa and 95 kDa respectively. As such, neither HA nor any other gadolinium based MRI agents administered intravenously are known to have any significant gastrointestinal uptake. The gastrointestinal

uptake we observed must be due to the unique structure of our HA–(EDA–DTPA–Gd) conjugates. HA is a highly negative charged molecule due to the presence of a carboxyl group in every repeating subunit. Incorporation of multiple $(DTPA-Gd)^{2-}$ groups to these carboxyl groups via EDA maintains these negative charges. These charges may have an impact on the distribution and excretion pattern of HA–(EDA–DTPA–Gd) conjugates. Additionally, we recognize the fact that, as a bifunctional chelate, DTPA dianhydride has been known crosslinking amines to form higher molecular weight polymeric aggregates (18). In the particular case of HA–EDA, DTPA dianhydride can produce both intramolecular and intermolecular crosslinking that results in polydispersed HA–EDA–DTPA conjugate products. Both types of crosslinking can change the linear structure of HA while intermolecular crosslinking also multiplies the molecular weight of the final conjugates. Both type of crosslinking may have profound influence on the HA–(EDA–DTPA–Gd) distribution and elimination, although size exclusive HPLC studies did not identify any higher molecular weight polymeric aggregates (supplemental material). We plan to use a bifunctional chelate with only one reactive functional group towards amines such as MX-DTPA (8) in the future to avoid any complication due to crosslinking.

5. CONCLUSION

HA–(EDA–DTPA–Gd) has been investigated as blood pool MR contrast agents. Agents based on HA of 16 and 74 kDa both show significant enhancement of the vasculature for an extended period of time. Clearance of the HA–(EDA–DTPA–Gd) conjugates based on 16 kDa HA followed a two-phase decay pattern, with a fast phase half-life at 12.4 min and a slow phase half-life at 141.2 min, which makes them potentially applicable to a range of MR studies including MRA and characterization of the tumor vasculature. Excretion rate of the HA–(EDA–DTPA–Gd) conjugates decreased as the HA molecular weight increased. Uptake in the stomach and lower gastrointestinal tract was observed for the HA–(EDA–DTPA–Gd) conjugates.

Supplementary Material

Refer to Web version on PubMed Central for supplementary material.

Acknowledgments

References

1. Maeda H, Fang J, Inutsuka T, Kitamoto Y. Vascular permeability enhancement in solid tumor: various factors, mechanisms involved and its implications. Int Immunopharmacol. 2003; 3(3):319–328. [PubMed: 12639809]

2. Goyen M. Gadofosveset-enhanced magnetic resonance angiography. Vasc Health Risk Manag. 2008; 4(1):1–9. [PubMed: 18629367]

3. Turetschek K, Floyd E, Helbich T, Roberts TP, Shames DM, Wendland MF, Carter WO, Brasch RC. MRI assessment of microvascular characteristics in experimental breast tumors using a new blood pool contrast agent (MS-325) with correlations to histopathology. J Magn Reson Imaging. 2001; 14(3):237–242. [PubMed: 11536400]

4. Baxter AB, Melnikoff S, Stites DP, Brasch RC. AUR Memorial Award 1991. Immunogenicity of gadolinium-based contrast agents for magnetic resonance imaging. Induction and characterization of antibodies in animals. Invest Radiol. 1991; 26(12):1035–1040. [PubMed: 1722486]

5. Bogdanov AA Jr, Weissleder R, Frank HW, Bogdanova AV, Nossif N, Schaffer BK, Tsai E, Papisov MI, Brady TJ. A new macromolecule as a contrast agent for MR angiography: preparation, properties, and animal studies. Radiology. 1993; 187(3):701–706. [PubMed: 8497616]

6. Frenzel T, Lengsfeld P, Schirmer H, Hutter J, Weinmann HJ. Stability of gadolinium-based magnetic resonance imaging contrast agents in human serum at 37 degrees C. Invest Radiol. 2008; 43(12):817–828. [PubMed: 19002053]

7. Sieber MA, Lengsfeld P, Frenzel T, Golfier S, Schmitt-Willich H, Siegmund F, Walter J, Weinmann HJ, Pietsch H. Preclinical investigation to compare different gadolinium-based contrast agents regarding their propensity to release gadolinium in vivo and to trigger nephrogenic systemic fibrosis-like lesions. Eur Radiol. 2008; 18(10):2164–2173. [PubMed: 18545998]

8. Franano FN, Edwards WB, Welch MJ, Brechbiel MW, Gansow OA, Duncan JR. Biodistribution and metabolism of targeted and nontargeted protein-chelate-gadolinium complexes: evidence for gadolinium dissociation in vitro and in vivo. Magn Reson Imaging. 1995; 13(2):201–214. [PubMed: 7739361]

9. Takakura Y, Mahato RI, Hashida M. Extravasation of macromolecules. Adv Drug Deliv Rev. 1998; 34(1):93–108. [PubMed: 10837672]

10. Mizuno N, Niwa T, Yotsumoto Y, Sugiyama Y. Impact of drug transporter studies on drug discovery and development. Pharmacol Rev. 2003; 55(3):425–461. [PubMed: 12869659]

11. Chong BF, Blank LM, McLaughlin R, Nielsen LK. Microbial hyaluronic acid production. Appl Microbiol Biotechnol. 2005; 66(4):341–351. [PubMed: 15599518]

12. Guillaumie F, Furrer P, Felt-Baeyens O, Fuhlendorff BL, Nymand S, Westh P, Gurny R, Schwach-Abdellaoui K. Comparative studies of various hyaluronic acids produced by microbial fermentation for potential topical ophthalmic applications. J Biomed Mater Res A. 2009

13. Kogan G, Soltes L, Stern R, Gemeiner P. Hyaluronic acid: a natural biopolymer with a broad range of biomedical and industrial applications. Biotechnol Lett. 2007; 29(1):17–25. [PubMed: 17091377]

14. Brown TJ. The development of hyaluronan as a drug transporter and excipient for chemotherapeutic drugs. Curr Pharm Biotechnol. 2008; 9(4):253–260. [PubMed: 18691086]

15. Esposito G, Geninatti Crich S, Aime S. Efficient cellular labeling by CD44 receptor-mediated uptake of cationic liposomes functionalized with hyaluronic acid and loaded with MRI contrast agents. ChemMedChem. 2008; 3(12):1858–1862. [PubMed: 18988207]

16. Platt VM, Szoka FC Jr. Anticancer therapeutics: targeting macromolecules and nanocarriers to hyaluronan or CD44, a hyaluronan receptor. Mol Pharm. 2008; 5(4):474–486. [PubMed: 18547053]

17. Schmiedl U, Ogan M, Paajanen H, Marotti M, Crooks LE, Brito AC, Brasch RC. Albumin labeled with Gd–DTPA as an intra-vascular, blood pool-enhancing agent for MR imaging: bio-distribution and imaging studies. Radiology. 1987; 162(1 Pt 1):205–210. [PubMed: 3786763]

18. Ogan MD, Schmiedl U, Moseley ME, Grodd W, Paajanen H, Brasch RC. Albumin labeled with Gd–DTPA. An intravascular contrast-enhancing agent for magnetic resonance blood pool imaging: preparation and characterization. Invest Radiol. 1987; 22(8):665–671. [PubMed: 3667174]

19. Shiftan L, Israely T, Cohen M, Frydman V, Dafni H, Stern R, Neeman M. Magnetic resonance imaging visualization of hyaluronidase in ovarian carcinoma. Cancer Res. 2005; 65(22):10316–10323. [PubMed: 16288020]

20. Gouin S, Winnik FM. Quantitative assays of the amount of diethylenetriaminepentaacetic acid conjugated to water-soluble polymers using isothermal titration calorimetry and colorimetry. Bioconjug Chem. 2001; 12(3):372–377. [PubMed: 11353534]

21. Kuo JW, Swann DA, Prestwich GD. Chemical modification of hyaluronic acid by carbodiimides. Bioconjug Chem. 1991; 2(4):232–241. [PubMed: 1772905]

22. Cowman MK, Matsuoka S. Experimental approaches to hyaluronan structure. Carbohydr Res. 2005; 340(5):791–809. [PubMed: 15780246]

23. Blundell CD, Deangelis PL, Almond A. Hyaluronan: the absence of amide-carboxylate hydrogen bonds and the chain conformation in aqueous solution are incompatible with stable secondary and tertiary structure models. Biochem J. 2006; 396(3):487–498. [PubMed: 16506956]

24. Stern R, Jedrzejas MJ. Hyaluronidases: their genomics, structures, and mechanisms of action. Chem Rev. 2006; 106(3):818–839. [PubMed: 16522010]

25. Harada H, Takahashi M. CD44-dependent intracellular and extracellular catabolism of hyaluronic acid by hyaluronidase-1 and -2. J Biol Chem. 2007; 282(8):5597–5607. [PubMed: 17170110]

26. Jackson DG. Immunological functions of hyaluronan and its receptors in the lymphatics. Immunol Rev. 2009; 230(1):216–231. [PubMed: 19594639]

27. Lebel L. Clearance of hyaluronan from the circulation. Adv Drug Deliv Rev. 1991; 7(2):221–235.

28. Geraldes CF, Laurent S. Classification and basic properties of contrast agents for magnetic resonance imaging. Contrast Media Mol Imag. 2009; 4(1):1–23.

29. Sherry AD, Cacheris WP, Kuan KT. Stability constants for Gd3+ binding to model DTPA-conjugates and DTPA-proteins: implications for their use as magnetic resonance contrast agents. Magn Reson Med. 1988; 8(2):180–190. [PubMed: 3210955]

30. Lebel L, Fraser JR, Kimpton WS, Gabrielsson J, Gerdin B, Laurent TC. A pharmacokinetic model of intravenously administered hyaluronan in sheep. Pharm Res. 1989; 6(8):677–682. [PubMed: 2813260]

31. Fraser JR, Laurent TC, Pertoft H, Baxter E. Plasma clearance, tissue distribution and metabolism of hyaluronic acid injected intravenously in the rabbit. Biochem J. 1981; 200(2):415–424. [PubMed: 7340841]

32. Nakabayashi H, Tsujii H, Okamoto Y, Nakano H. Fluorescence-labeled-hyaluronan loading test as an index of hepatic sinusoidal endothelial cell function in the rat. Int Hepatol Commun. 1996; 5(6):345–353.

33. Mochizuki S, Kano A, Shimada N, Maruyama A. Uptake of enzymatically-digested hyaluronan by liver endothelial cells in vivo and in vitro. J Biomater Sci Polym Ed. 2009; 20(1):83–97. [PubMed: 19105902]
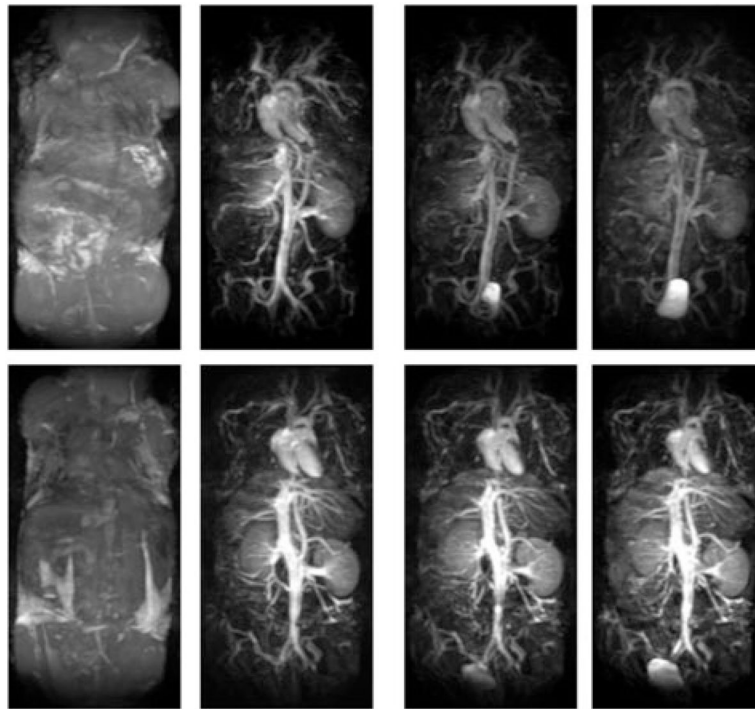
Figure 1.
Coronal maximum intensity projection (MIP) of the 3D FLASH images obtained from the mice injected with HA–(EDA–DTPA–Gd) at 0.1 mmol Gd kg^{-1}. Pre-contrast and 0, 10 and 30 min post contrast images are shown from left to right. Post-contrast images are shown here after the subtraction of the corresponding pre-contrast images. Top images are from 16 kDa HA and lower images are from 74 kDa HA.
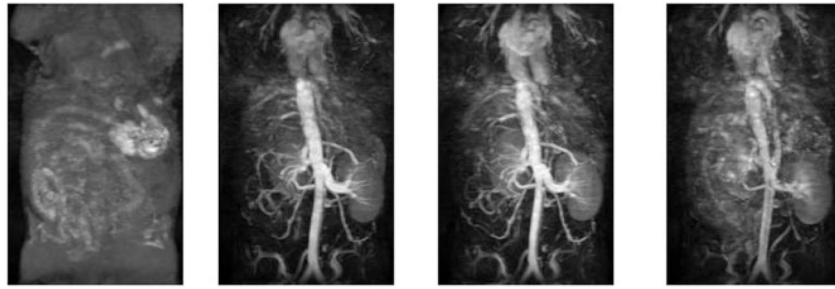
Figure 2.
Coronal MIP of the 3D FLASH images obtained from a mouse injected with BSA–(DTPA–Gd) at 0.1mmol Gd kg^{-1}. Pre-contrast and 0, 10 and 30 min post contrast images are shown from left to right. Post-contrast images are shown here after the subtraction of the corresponding pre-contrast images.
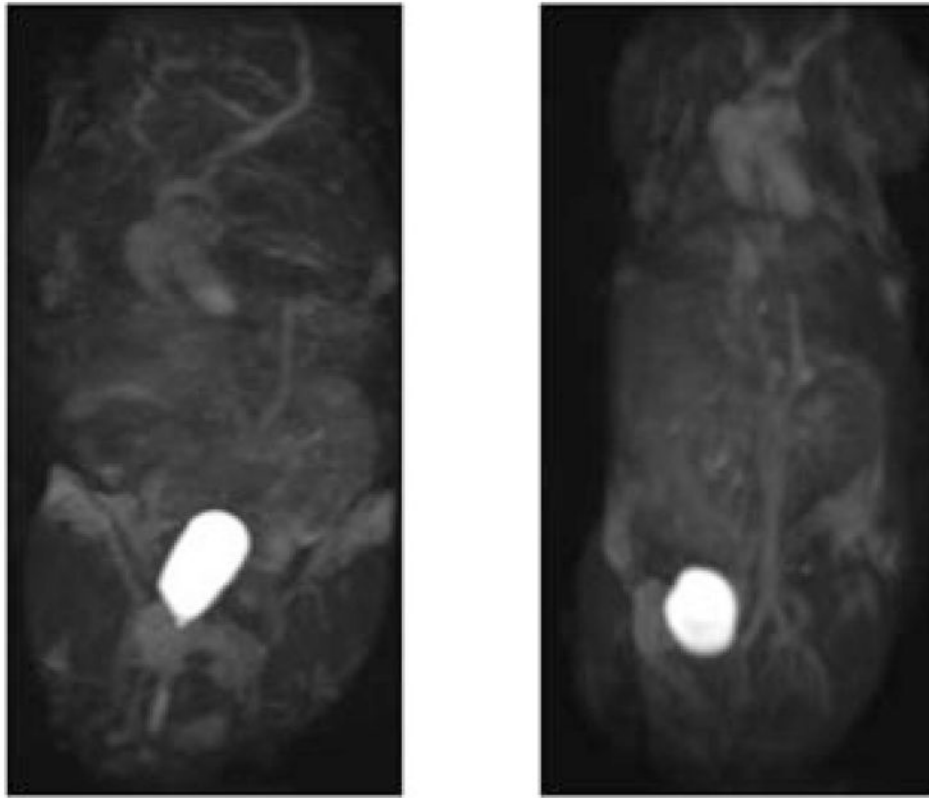
Figure 3.
Coronal MIP of the 3D FLASH images obtained from the mice injected with HA–(EDA–DTPA–Gd) at 150 min post injection. Left image is from 16 kDa HA and right image is from 74 kDa HA.
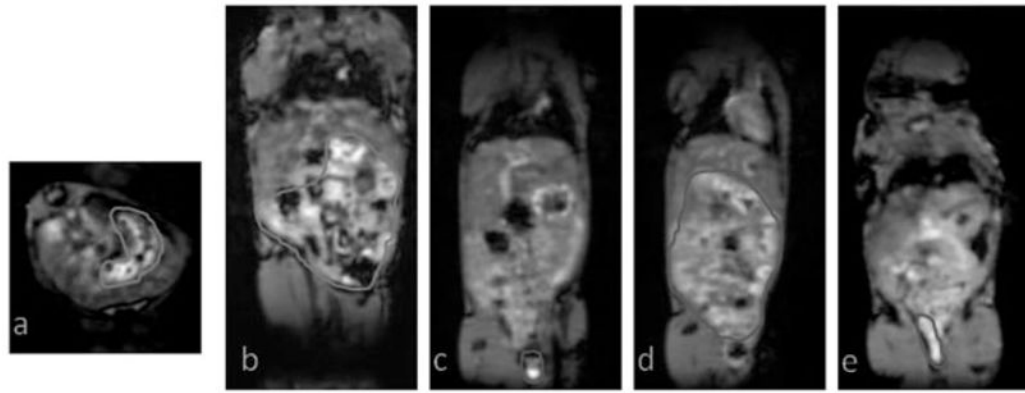
Figure 4.
3D FLASH images obtained from a mouse injected with 16 kDa HA–(EDA–DTPA–Gd), areas with gadolinium uptakes are highlighted. (a, b) Axial and coronal images showing the stomach and lower gastrointestinal uptake at 1 h post injection. (c, d) Coronal images showing the lower gastrointestinal and feces uptake at 7 h post injection. (e) A coronal image showing the presence of gadolinium enhancement in the feces at 24 h.
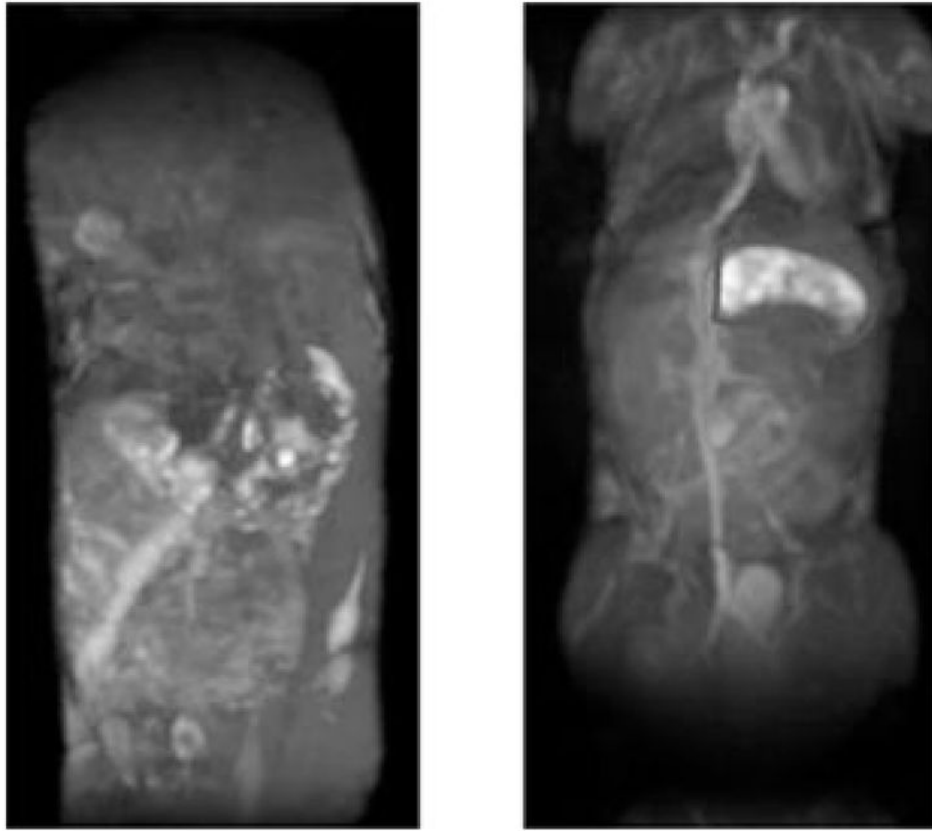
Figure 5.
Coronal MIP of the 3D FLASH images obtained from the mice injected with HA–(EDA–DTPA–Gd) at 24 h post injection. Left image is from 16 kDa HA and right image is from 74 kDa HA. Highlighted area shows the stomach uptake of 74 kDa HA–(EDA–DTPA–Gd).
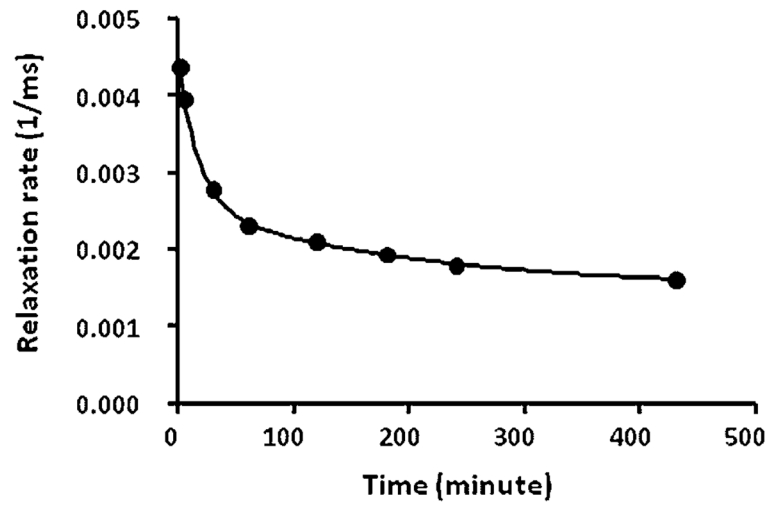
Figure 6.
Blood relaxation rate as a function of time of a mouse injected with 16 kDa HA–(EDA–DTPA–Gd).

Table 1

T_1 values (at 1.3 mg ml^{-1}) and relaxivity of HA–(EDA–DTPA–Gd) of different molecular weight at 25°C, measured at 1.5 and 9.4 T, at which water T_1 is 2.5 and 2.8 s

	1.5T		9.4T	
MW of HA (kDa)	16	74	16	74
T_1 values (s)	0.418	0.417	0.490	0.470
Gd content (% weight)	4.5	5.2	4.5	5.2
Gd Concentration (mM)	0.37	0.43	0.37	0.43
Relaxivity [mM(Gd)$^{-1}$s^{-1}]	5.38	4.65	4.55	4.12

Table 2

Stability of HA–(EDA–DTPA–Gd) conjugate in RPMI medium (4 mg ml^{-1}) with 10% FBS at various pH, measured as T_1 (ms) up to 5 days

Time (h)	T_1 (ms)		
	pH = 6.3	pH = 7.4	pH = 9.0
0.05	176	194	190
1	178	197	191
2	183	196	194
24	186	208	202
50	190	212	206
123	201	221	220